ELSEVIER

Contents lists available at ScienceDirect

Scripta Materialia

journal homepage: www.journals.elsevier.com/scripta-materialia



The dual effect of surface adsorbates on fracture of calcite

Derek H. Warner a,b,*, Scott J. Grutzik c, Anastasia G. Ilgen d

- ^a Canterbury Fracture Group, Civil and Natural Resources Engineering, University of Canterbury, Christchurch, 8041, New Zealand
- ^b Cornell Fracture Group, School of Civil and Environmental Engineering, Cornell University, Ithaca NY 14853, USA
- ^c Materials and Failure Modeling Department, Sandia National Laboratories, Albuquerque, NM 87185, USA
- ^d Geochemistry Department, Sandia National Laboratories, Albuquerque, NM 87185, USA

ARTICLE INFO

Keywords: Environmental effects Impurities Ions Failure Atomistic modeling

ABSTRACT

Harnessing ab-initio electronic structure calculations, this study reveals the role of surface adsorbates on the tendency of brittle fracture - a key failure mode of minerals such as calcite. The results demonstrate that (1) adsorbates can both enhance and inhibit the tendency to fracture, depending on the bonding configuration of the adsorbate to the calcite surface, and (2) the disassociation/reaction of water at the surface substantially enhances its degrading effect on fracture. This establishes the feasibility for tuning in either direction the tendency of brittle minerals to fracture by manipulating the composition of secondary elements in environments and materials.

The presence of minute chemical species from the environment can have catastrophic consequences in both natural and engineered load bearing structures. In many cases, the mechanism by which environmental species act to influence fracture is not established; and thus, engineers are faced with considerable uncertainty when designing for contexts where empirical data does not exist. Beyond unforeseen failures, this lack of understanding leads to the use of overly conservative and inefficient safety factors, while also inhibiting the design and adoption of new technologies.

The mechanical integrity of calcite, $CaCO_3$, provides a prime example. Calcite is one of the most abundant minerals in the Earth's crust, plays a key role in numerous biological processes [1] and the inorganic carbon cycle, and has been central to many technological innovations in geoengineering. Across these contexts, the mechanical integrity of calcite can be a governing concern. Applications of subsurface hydrogen, compressed air, and CO_2 storage, are timely technological examples, where subsurface fractures are key to the transport and reaction rates of geologically stored compounds [2]. Reaction and transport rates ultimately govern economics, safety, and viability of subsurface storage [3,4].

Laboratory studies of calcite fracture have involved a myriad of conditions, dating back at least three decades [5–7]. The most recent studies [8,9] highlight multiple environmental effects. First, the presence of water (in liquid or vapor form) enhances fracture. Second, the tendency to fracture in water can be sensitive to the presence of specific anions, but not changes in pH or the rate of dissolution. When the presence

ence of anions is of consequence, fracture is inhibited upon the addition of anions to deionized water.

Of the above effects, the increased tendency for fracture in water is the most widely acknowledged [7,8]. Consequently, it is natural to hypothesize that the observed inhibition of fracture by anions is due to anions protecting the calcite surface from the water [8,9]. Here, the molecular-scale basis for this hypothesis is examined, as well as the more general question of how and why do adsorbates affect the fracture of calcite?

Experimental methodologies capable of isolating individual contributions to the extent needed to answer these questions have yet to be established, and direct microscopic observation at the scales needed remains out of reach [10–16]. This leaves atomic-scale computer modeling as perhaps the most capable tool to characterize the action of environmental fracture mechanisms. Here, ab-initio electronic structure calculations were utilized to answer the above question and to more generally provide a basis for understanding environmental effects. The central finding is the demonstration that adsoption can have a dual role. It can both enhance and inhibit fracture, leading to a complexity that has likely contributed to the long-standing challenge of accurately predicting macroscopic fracture behavior from atomic-scale processes [17,18]. That said, the complexity revealed here also presents an opportunity for atomic-scale design of fracture behavior via control of environment and material composition.

This study utilizes the Density Functional Theory electronic structure method [19,20] to obtain meaningful atomic configurations of

https://doi.org/10.1016/j.scriptamat.2023.115952

^{*} Corresponding author at: Canterbury Fracture Group, Civil and Natural Resources Engineering, University of Canterbury, Christchurch 8041, New Zealand. E-mail address: derek.warner@canterbury.ac.nz (D.H. Warner).

calcite in bulk, slab, and rod forms (Fig. S1), with and without surface adsorbates. The energy difference between the slab and bulk (or rod and slab) configurations can be interpreted as a cleavage energy, ΔE , associated with the rupture of bonds across a cleavage plane. Accordingly, ΔE provides an indicator of the tendency to fracture, which in the terminology of fracture mechanics is characterized as a fracture toughness [21], K_{IC} . In the limit of an ideally brittle material with a homogeneous cleavage energy density on the fracture plane and no lattice trapping [22], K_{IC} can be expressed as

$$K_{IC} = \sqrt{2C\frac{\Delta E}{A}},\tag{1}$$

with \mathcal{C} being an elastic constant and A being the surface area created by cleavage. Thus, the expected change in fracture toughness resulting from the changes in the cleavage energies reported here will be moderated by a square root operator. They will also scale with the concentration of the adsorbates along the crack tip.

The electronic structure was modeled using the Kohn-Sham Density Functional Theory approach [20] with the Born-Oppenheimer approximation [23] as implemented in the Vienna Ab initio Simulation Package (VASP 5.4.4.18) [19]. The exchange-correlation energy was modeled using the Perdew-Burke-Ernzerhof [24] (PBE) generalized gradient approximation (GGA). Physical phenomena beyond the PBE exchange-correlation model were not explicitly considered [25] and are left for future studies, e.g. dispersion [26,27]. To keep the modeling computationally tractable, the projector augmented wave (PAW) potentials given in Table S1 were used. Forces were calculated from the electronic structure using the Hellmann–Feynman theorem [28]. The model was discritized using plane wave basis with an energy cut-off of 520 eV. Gaussian smearing of 0.05 eV was used in all calculations.

Central to this study is a slab configuration derived from a relaxed primitive rhombohedral unit cell of a calcite lattice, shown in Fig. S2. The relaxed primitive cell was obtained by optimizing the cell degrees of freedom to an energy tolerance of 0.01 meV. The electronic structure for these calculations was obtained by integrating the irreducible part of the Brillouin zone with a grid of 13 Gamma-centered k-points. This relaxed primitive cell had dimensions of $\alpha = 46.15^{\circ}$ and a = 6.447 Å. The $[20\overline{1}]$, $[\overline{1}02]$, and $[1\overline{3}1]$, lattice vectors of the primitive cell were then used as basis vectors to create the supercell slab geometry. The supercell had boundaries parallel to the (211), (112), and $(0\overline{1}0)$ planes, with the first two belonging to the family of commonly observed calcite cleavage planes [29,30]. The hexagonal representation of calcite is often referenced in literature as it provides a clear view of calcite's alternating layers of carbonate and calcium atoms, and a clear perspective of the nonpolar nature of the cleavage plane. With respect to the hexagonal unit cell, the cleavage plane is expressed as {1014}.

The supercell slab geometry consisted of a lattice of two periodic lengths along the [201] direction and one periodic length along the [102] and [131] directions. The [102] basis vector was extended 20 Å beyond the lattice to create the slab-vacuum geometry, consisting of two {211} surfaces separated by three layers of atoms (Fig. 1). The further extension of each of the basis vectors and lattice by one periodic unit returned an energy within 4 meV for a test case that included a Cl adatom. This provides a measure of periodic cell effects.

The aforementioned geometry is convenient for this study as the extension of the $[20\bar{1}]$ basis vector converts the slab to a rod geometry with four $\{211\}$ surfaces. The transition from slab to rod can be interpreted as a cleavage event on the experimentally observed (211) cleavage plane that intersects a (112) surface. In that spirit, the calculations presented here give insight into the occurrence of mixed mode cleavage at a blunted crack tip (Fig. 2). The blunted configuration has been chosen as a limiting case, where impurity access to crack tip bonds is not constrained by a narrow crack geometry. In slab and rod geometries, the electronic structure was obtained from a single Gamma-centered k-point.

Four bonds per lattice period span the $(2\,1\,1)$ cleavage plane at the $(1\,1\,2)$ slab surface. In all cases, the bonds are between Ca and O atoms. The Ca atoms lie on a common $(1\,1\,2)$ surface plane. Two of the Ca-O bonds lie within this plane, one drops below it into the bulk, and the other rises out of it (Fig. 2). These three cases of surface Ca-O bonds will subsequently be referred to as the α , β , and γ bonds, respectively.

All Ca atoms on the (112) surface have reduced nearest neighbor coordination relative to their bulk state, i.e. five nearest neighbor bonds as apposed to six. Three fourths of the O atoms at the surface have bulk nearest neighbor coordination. The O atoms that do not have bulk coordination, i.e. have two nearest neighbor bonds as opposed to three, are associated with γ Ca-O bonds across the cleavage plane.

Six distinct surface adsorbate geometries were examined (Fig. S3):

- H bonded to the under coordinated O atom of the γ bond to assess the effect of H on cleavage energy,
- OH, Cl, and SO₄ bonded to the Ca atom of the α bond to assess the
 effect of OH, Cl, and SO₄ on cleavage energy,
- H₂O bound to the Ca atom of the α bond to assess the effect of H₂O on cleavage energy, and more generally the effect of an adsorbate that is not ionically or covalently bonded.
- Cl bonded to the surface Ca atom of the γ bond to assess the effect of binding site on cleavage energy,
- SO₄ bonded to a Ca atom of a α bond and the Ca atom of the β bond on the opposite side of the (112) cleavage plane to assess bidentate binuclear configurations;
- H₂O bound to a Ca atom of the α bond that spans the cleavage plane and an O atom of a γ bond that does not span the cleavage plane, to assess a bidentate binuclear configuration that is distinctly different than the above case;

The majority of cases were examined in two contexts, i.e. a vacuum environment at the (112) slab surface and a structured double layer of water. In all cases, the initial slab geometry was obtained by minimizing the forces on all atoms on and above the top surface layer of calcite to a 10 meV/Å tolerance. In each step of the structural minimization, the electronic structure was converged to 0.001 meV, noting that less demanding tolerances were found to produce electronic structures that were dependent upon the minimization scheme and initial guess in some cases. The mononuclear SO₄ configuration is an intermediate configuration obtained during the atomic minimization from a mononuclear SO₄ starting guess. The single mononuclear water molecule configuration is unstable and was simulated without atomic minimization. This configuration was created by removing all but one water molecule from the minimized water double layer structure. The results of the unrelaxed single mononuclear water molecule configurations were consistent with the minimized double layer simulations, and were thus viewed to be meaningful. In all cases reported herin, the cleavage energies correspond to a rigid cleavage energy, whereby the atomic positions are held fixed as simulation cell is expanded. Further details of the configurations and methods are given in the supplementary materials.

With the above preliminaries in place, we begin by comparing the rigid cleavage energy of the slab and bulk configurations. Cleaving the bulk configuration requires less energy than cleaving the slab configuration. For the specific case of simulation cells simulated here, composed of three atomic columns across the fracture plane (Fig. S1), cleavages energies of $\Delta E=7.19$ eV for the bulk and $\Delta E=9.50$ eV for the slab were obtained. In a mode I plane stress scenario, the bulk result corresponds to $K_{IC}=0.21$ MPa \sqrt{m} , in the limit of equation (1) with $C\approx97$ GPa in the direction normal to the cleavage plane using the laboratory measured room temperature anisotropic elastic constants of calcite [31]. For comparison, laboratory measured values of calcite crystals are in the range of 0.10 - 0.16 MPa \sqrt{m} at room temperature in laboratory air [8].

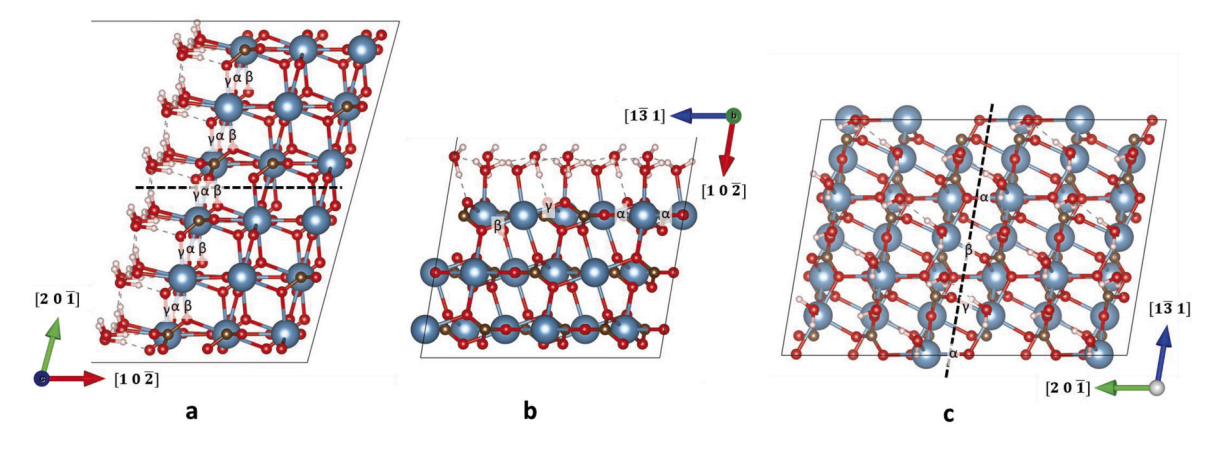


Fig. 1. View of relaxed calcite slab configuration with water double layer from three orientations. The three types of surface Ca-O bonds referenced in the text, i.e. γ , α , and *beta* are labeled. In a and c, the (211) calcite cleavage plane is visable and highlighted with a bold dashed line. Atomic coloring of blue - Ca, red - O, brown - C, and white - H. (For interpretation of the colors in the figure(s), the reader is referred to the web version of this article.)

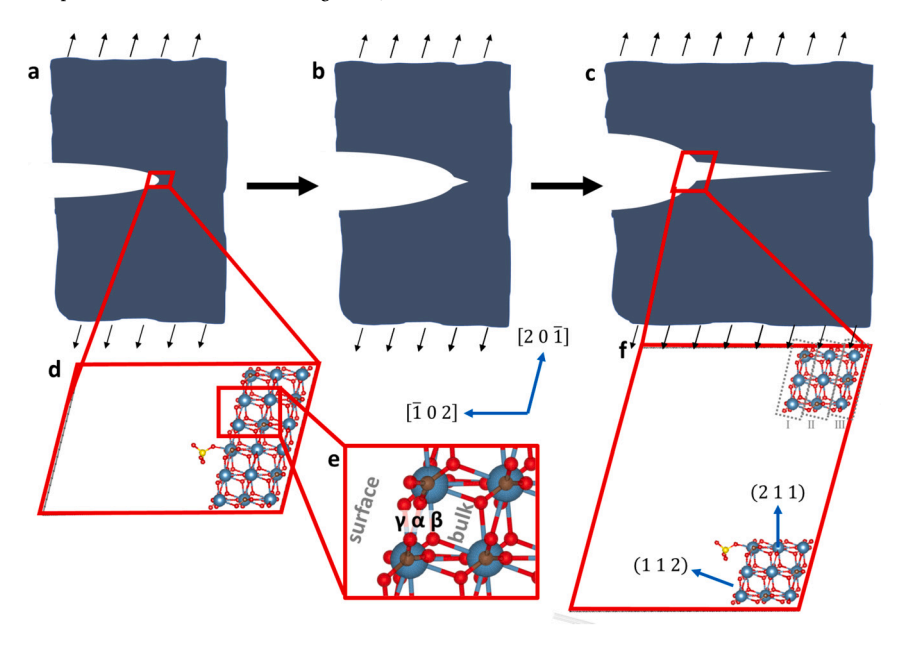


Fig. 2. Images a, b, and c, illustrate sequential configurations of cleavage fracture initiated from a blunt crack tip. d displays a simulation cell with a calcite slab and a mononuclear SO_4 adsorbate and is intended to represent the atomic configuration at the blunted crack tip in a. e displays a zoomed view of d that shows the three types of Ca-O bonds at the outermost surface layer. A larger view of e is available in Fig. S6. f displays a simulation cell with a calcite rod configurations having a mononuclear SO_4 adsorbate and is intended to represent the atomic configuration at a cleaved blunted crack tip as shown in c. The directions and Miller indices of planes are given with respect to the basis vectors of the Rhombohedral calcite primitive unit cell.

The increased cleavage energy of the slab configuration can be attributed to an effect that is localized to the Ca-O bonds nearest the preexisting surface of the slab. This is deduced by partitioning ΔE across the atomic columns spanning the cleavage plane via a force integration approach that is described in the supplementary material. Following the labeling in Fig. 2f, partitioned cleavage energies of 3.60, 2.40, and 3.59 eV are found for slab columns I, II, and III respectively. These energies contrast the bulk configuration, where each column has the same partitioned cleavage energy of 2.40 eV. The consistent value of column II among the bulk and slab cases establishes that the effect of the prexisting surface on cleavage energy is due to the outer most layer of atoms and their Ca-O bonds that span the cleavage plane. This finding is consistent with the traditional understanding of bonding [32], whereby atoms with reduced nearest-neighbor coordination are more strongly bonded to their neighbors.

Focusing first on mononuclear [33] adsorbate configurations, single adsorbates lower the cleavage energy of the slab by 0.43 - 0.48 eV, in the examined cases of Cl, OH, SO₄, and H (Fig. 3). In these cases, the

Cl, OH, and SO_4 are ionically bonded to a surface Ca atom that has a Ca-O bond across the cleavage plane (labeled as α in Fig. 2). In the case of H, the adsorbate is covalently bonded to a surface O atom having a Ca-O bond across the cleavage plane (labeled as γ in Fig. 2). Force integration reveals that this effect is localized to the outermost calcite surface layer of Ca, C, and O atoms. It is noteworthy that despite a significant variation in Bader charge [34] among the adsorbates (-0.55, -0.43, -0.72, and +0.58) they have a similar effect on cleavage. In the case of a single water mononuclear adsorbate bonded to a surface Ca atom, the result is significantly different.

In contrast to the previous cases, the charge neutral mononuclear water adsorbate does not transfer electrons or form a covalent bond with the calcite. Instead, it is bound by a dipole-dipole interaction between the O of the water molecule and the surface Ca atom, a configuration that has been observed elsewhere in the literature [35]. In this case, the rigid cleavage energy decreases by only 0.05 eV due to the presence of the water molecule at the surface Ca. In the case of a structured layer of water molecules (which is discussed in later paragraphs

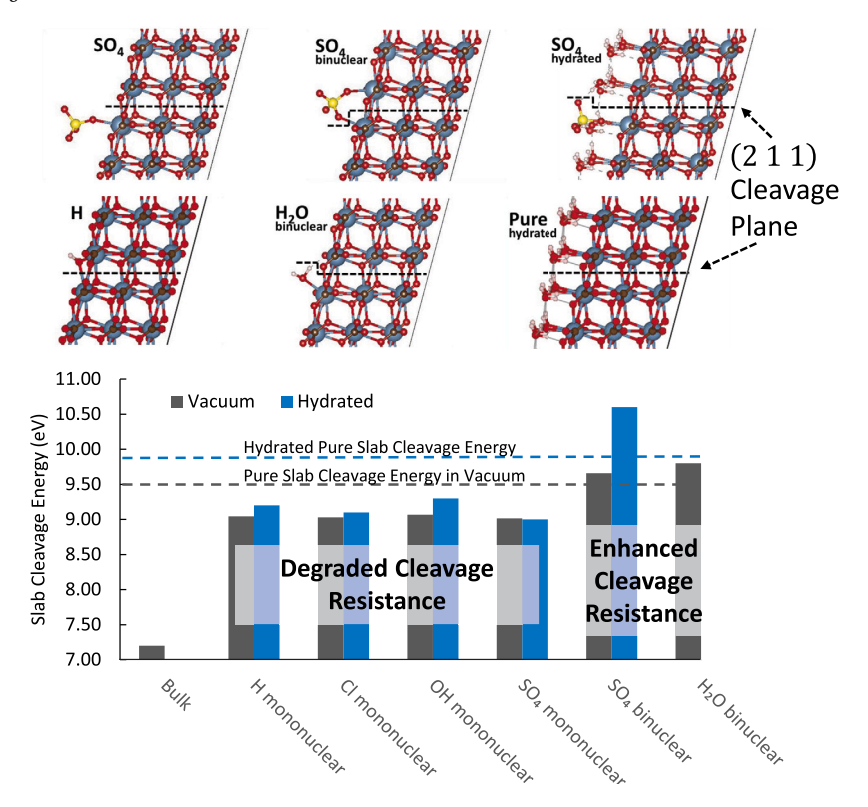


Fig. 3. Top: Zoomed images from selected relaxed calcite slab configurations. See supplementary figures for complete set of configurations. The black dashed line represents the plane across which cleavage acted in each case. Atomic coloring of blue - Ca, red - O, brown - C, white - H, yellow - S, and green - Cl. Bottom: Calculated energy to cleave calcite simulation cells along dashed black line. Gray bars correspond to slab configurations in vacuum with a single adsorbate and blue bars correspond to slab with hydrated surface. Bulk cleave energy is shown as a reference.

and presented in Figs. 3 and S4), the effect is increased nearly proportionally to the number of water molecules (8) bound to the surface Ca and O atoms with bonds spanning the cleavage plane. Together with the results of the previous paragraph, the calculations presented thus far suggest that when water molecules disassociate/react on a surface, they can have a much more substantial impact on cleavage relative to binding in their associated state. This provides support for a long held hypothesis of crack tip chemomechanics [36], and is thus a key result of the paper. In the case of calcite, such a disassociation reaction is expected [29] at surface defects, e.g. steps, and may be a key contributor to fracture initiating from such defects.

The simulation results presented to this point display two trends that diverge from experimental observations [8,9]: (1) of the adsorbates considered, pure water in its associated state exhibits the least detrimental effect on fracture, (2) among the remaining adsorbates which chemically bound to the calcite surface, their type does not have a significant effect. That said, the results do align with fundamental bonding principles, where higher coordination corresponds to reduced binding strength [32].

In the case of SO_4 , a simple explanation was observed, via extensive structural relaxation. The structural relaxation revealed the existence of a lower energy binuclear [33] adsorbate configuration for SO_4 . This configuration can bridge the cleavage plane, increasing the number of bonds that must be broken for a cleavage event to occur. Thus, while the adsorption of SO_4 to calcite decreases the binding of the calcite bonds across the cleavage plane, it increases the number of bonds that must be broken, and ultimately increases the cleavage energy by 0.16 eV. The net increase in calculated cleavage energy of the binuclear configuration provides a consistency with the experimentally observed trend of increased fracture resistance with the addition of SO_4 to the environment.

The increase of cleavage energy due to adsorption is not unique to SO_4 . It was also observed for a single water molecule adsorbate in a fully

relaxed configuration, whereby it bonded with the Ca and O surface atoms in a binuclear configuration. When this configuration spans the cleavage plane, the cleavage energy increased by 0.32 eV. The tendency of the SO_4 and water molecule to form binuclear configurations that can inhibit fracture, while the H, OH, and Cl do not, may be attributed to the larger size of the SO_4 and water molecules, which allows them to easily bind to the calcite in two locations. A full exploration of the possibility of OH forming a binuclear configuration remains to be explored.

The concept of adsorbates spanning the cleavage plane and enhancing cleavage resistance extends beyond binuclear adsorbates. When the calcite surface is saturated by water, a structured double layer of water molecules form, whereby each water molecule is bound to the calcite surface in a mononuclear configuration [29,37,38]. The double layer spans the cleavage plane and cleaves together with the calcite. While the presence of the water layer does reduce the cleavage energy within the calcite, the reduction is more than offset by the additional cleavage energy required to cleave the water layer itself.

Given that this result is in contrast to experimental observations that suggest that water reduces cleavage resistance [7], it is reasonable to hypothesize that a structured layer of associated water molecules does not exist at the crack tip, making the simulations discussed here disconnected from the real-world situation [7]. Nonetheless, this does not diminish the takeaway point that adsorbate films can increase fracture resistance, even when the individual adsorbate molecules are weakly bound in mononuclear configurations via dipole-dipole interaction. Managing the disruption of such films by controlling chemical heterogeneity and surface defects, might then be a strategy for altering fracture properties.

Regarding the effects of pH, the results shown in Fig. 3 suggest that both increases and decreases in pH from neutral would decrease cleavage energy. Specifically, both H and OH decrease cleavage energy more than water. This is not aligned with the results of fracture experiments [8], where the effect of solution pH is indiscernible over a

substantial range about the neutral value of 7. The resolution to this discrepancy is straight forward in that the pH of a surface water layer has been shown to be largely independent of the pH of the solution [39].

In summary, laboratory studies [8,9] suggest that water enhances fracture and that the enhancement can be inhibited by the presence of specific anions in the solution, e.g. SO_4 and Cl . In accord, the modeling presented here suggests that an unstructured water layer will enhance fracture, and that if water were to disassociate at the crack tip, it would have an even greater enhancing effect. The presence of SO_4 in a binuclear configuration will inhibit such enhancement, either by directly increasing the cleavage energy or by inducing crack deflection [40]. In contrast, the modeling did not show discernible enhancement with Cl , and in this way is inconsistent with the cited laboratory work [8,9]. This suggests the operation of mechanisms having greater complexity than examined here in the case of Cl .

Ultimately, the interplay of environmental factors on the cleavage process of calcite and, by extension, other brittle materials, has been found to exert both amplifying and detractive effects. The simulations indicate that modifications in composition, even minor ones, can alter surface properties. This can result in the reduction of individual bond strength across the cleavage plane, while potentially augmenting the count of bonds spanning the same plane. Despite the many simplifications of the modeling relative to real calcite-adsorbate systems, these are robust concepts that are unlikely to change with more complete analyses.

Not only do these results elucidate the origin of intricate environmental effects observed at the macroscopic scale, they also suggest strategies for nanoscale optimization of environmental conditions and material composition. Beyond enhancing control over the tendency towards brittle fracture, the findings may bear relevance to intrinsically ductile materials that emit dislocations from crack tips [41–43], with application to both static and fatigue loading [18]. In the intrinsically ductile case, plastic slip breaks surface bonds and creates new surface at a slip step. The breaking of such surface bonds might be impacted by environmental conditions and material composition in similar ways to the brittle calcite material studied here, particularly when one considers cases involving the presence of nonmetallic surface films.

Declaration of competing interest

The authors declare that they have no known competing financial interests or personal relationships that could have appeared to influence the work reported in this paper.

Acknowledgements

The authors thank K. Leung for reviewing a draft of the manuscript and providing valuable technical insight. The work was supported by the laboratory directed research and development program at Sandia National Laboratories (project # 222398). This article has been authored by employees of National Technology and Engineering Solutions of Sandia, LLC under Contract No. DE-NA0003525 with the U.S. Department of Energy (DOE). The employees own all right, title and interest in and to the article and are solely responsible for its contents. The United States Government retains and the publisher, by accepting the article for publication, acknowledges that the United States Government retains a non-exclusive, paid-up, irrevocable, world-wide license to publish or reproduce the published form of this article or allow others to do so, for United States Government purposes. The DOE will provide public access to these results of federally sponsored research in accordance with the DOE Public Access Plan https://www.energy.gov/downloads/doepublic-access-plan. This paper describes objective technical results and analysis. Any subjective views or opinions that might be expressed in the paper do not necessarily represent the views of the U.S. Department of Energy or the United States Government. DHW gratefully acknowledges support from the Office of Naval Research #N000142012484 and the National Science Foundation #1922081.

OpenAI's language model, ChatGPT, was utilized in the refinement of the text. After using this tool, the authors reviewed and edited the content and take full responsibility for the content of the publication.

Appendix A. Supplementary material

Supplementary material related to this article can be found online at https://doi.org/10.1016/j.scriptamat.2023.115952.

References

- J.W. Dunlop, P. Fratzl, Multilevel architectures in natural materials, Scr. Mater. 68 (2013) 8–12.
- [2] N. Kampman, et al., Observational evidence confirms modelling of the long-term integrity of co2-reservoir caprocks, Nat. Commun. 7 (2016) 12268.
- [3] J. Rutqvist, The geomechanics of co 2 storage in deep sedimentary formations, Geotech. Geolog. Eng. 30 (2012) 525–551.
- [4] A.S. Lord, et al., Overview of geologic storage of natural gas with an emphasis on assessing the feasibility of storing hydrogen, in: M. Bui, N. Mac Dowell (Eds.), OSTI, 2009, https://www.osti.gov/servlets/purl/975258-OsnNqC/.
- [5] J. Dunning, B. Douglas, M. Miller, S. McDonald, The role of the chemical environment in frictional deformation: stress corrosion cracking and comminution, Pure Appl. Geophys. 143 (1994) 151–178.
- [6] F. Rostom, A. Røyne, D.K. Dysthe, F. Renard, Effect of fluid salinity on subcritical crack propagation in calcite. Tectonophysics 583 (2013) 68–75.
- [7] A. Royne, J. Bisschop, D.K. Dysthe, Experimental investigation of surface energy and subcritical crack growth in calcite, J. Geophys. Res., Solid Earth 116 (2011) 1–10.
- [8] A.G. Ilgen, et al., Chemical controls on the propagation rate of fracture in calcite, Sci. Rep. 8 (2018) 1–13.
- [9] R.C. Choens, J. Wilson, A.G. Ilgen, Strengthening of calcite assemblages through chemical complexation reactions, Geophys. Res. Lett. 48 (2021) e2021GL094316.
- [10] S.P. Lynch, Environmentally assisted cracking: overview of evidence for an adsorption-induced localised-slip process, Acta Metall. 36 (1988) 2639–2661.
- [11] S.M. Ohr, An electron microscope study of crack tip deformation and its impact on the dislocation theory of fracture, Mater. Sci. Eng. 72 (1985) 1–35.
- [12] I.M. Robertson, H.K. Birnbaum, An HVEM study of hydrogen effects on the deformation and fracture of nickel, Acta Metall. 34 (1986) 353–366.
- [13] G.M. Bond, I.M. Robertson, H.K. Birnbaum, The influence of hydrogen on deformation and fracture processes in high-strength aluminum alloys, Acta Metall. 35 (1987) 2289–2296.
- [14] G.O. Ilevbare, O. Schneider, R.G. Kelly, J.R. Scully, In situ confocal laser scanning microscopy of AA 2024-t3 corrosion metrology: I. Localized corrosion of particles, J. Electrochem. Soc. 151 (2004) B453.
- [15] A. Turnbull, Corrosion pitting and environmentally assisted small crack growth, Proc. R. Soc. A, Math. Phys. Eng. Sci. 470 (2014).
- [16] T.J. Stannard, et al., 3d time-resolved observations of corrosion and corrosion-fatigue crack initiation and growth in peak-aged al 7075 using synchrotron x-ray tomography, Corros. Sci. 138 (2018) 340–352.
- [17] E. Bitzek, J.R. Kermode, P. Gumbsch, Atomistic aspects of fracture, Int. J. Fract. 191 (2015) 13–30.
- [18] M. Zhao, G. Wenjia, D.H. Warner, Atomic mechanism of near threshold fatigue crack growth in vacuum, Nat. Commun. 13 (2022) 1–10.
- [19] G. Kresse, J. Hafner, Ab initio molecular dynamics for open-shell transition metals, Phys. Rev. B 48 (1993) 13115–13118.
- [20] W. Kohn, L.J. Sham, Self-Consistent equations including exchange and correlation effects, Phys. Rev. 140 (1965) A1133–A1138.
- [21] A.T. Zehnder, Lecture notes on fracture mechanics, Cornell Univ. 20 (2007) 22.
- [22] N. Bernstein, D.W. Hess, Lattice trapping barriers to brittle fracture, Phys. Rev. Lett. 91 (2003) 25501.
- [23] M. Born, R. Oppenheimer, Zur Quantentheorie der Molekeln, Ann. Phys. 389 (1927) 457–484.
- [24] J.P. Perdew, K. Burke, M. Ernzerhof, Generalized Gradient approximation made simple, Phys. Rev. Lett. 77 (1996) 3865–3868.
- [25] X. Cheng, Y. Zhang, E. Jónsson, H. Jónsson, P.M. Weber, Charge localization in a diamine cation provides a test of energy functionals and self-interaction correction, Nat. Commun. 7 (2016).
- [26] E. Ataman, M.P. Andersson, M. Ceccato, N. Bovet, S.L. Stipp, Functional group adsorption on calcite: I. Oxygen containing and nonpolar organic molecules, J. Phys. Chem. C 120 (2016) 16586–16596.
- [27] M.P. Andersson, K. Dideriksen, H. Sakuma, S.L. Stipp, Modelling how incorporation of divalent cations affects calcite wettability-implications for biomineralisation and oil recovery, Sci. Rep. 6 (2016) 1–14.
- [28] R.P. Feynman, Forces in molecules, Phys. Rev. 56 (1939) 340–343.
- [29] S. Kerisit, S.C. Parker, J.H. Harding, Atomistic simulation of the dissociative adsorption of water on calcite surfaces, J. Phys. Chem. B 107 (2003) 7676–7682.

- [30] A.J. Skinner, J.P. Lafemina, H.J. Jansen, Structure and bonding of calcite: a theoretical study, Am. Mineral. 79 (1994) 205–214.
- [31] G. Ulian, D. Moro, G. Valdrè, Elastic properties of heterodesmic composite structures: the case of calcite caco3 (space group r3-c), Comp. Part C: Open Access 6 (2021) 100184
- [32] V. Heine, et al., Many-atom interactions in solids, Philos. Trans. R. Soc., Math. Phys. Eng. Sci. 334 (1997) 393–405.
- [33] A.C. Ladeira, V.S. Ciminelli, H.A. Duarte, M.C. Alves, A.Y. Ramos, Mechanism of anion retention from EXAFS and density functional calculations: Arsenic (V) adsorbed on gibbsite, Geochim. Cosmochim. Acta 65 (2001) 1211–1217.
- [34] R.F. Bader, Atoms in molecules, Acc. Chem. Res. 18 (1985) 9-15.
- [35] J.S. Lardge, D.M. Duffy, M.J. Gillan, Investigation of the interaction of water with the calcite (10.4) surface using ab initio simulation, J. Phys. Chem. C 113 (2009) 7207–7212.
- [36] T.A. Michalske, B.C. Bunker, Stress corrosion of ionic and mixed ionic/covalent solids, J. Am. Ceram. Soc. 69 (1986) 721–724.
- [37] P. Fenter, S.S. Lee, Hydration layer structure at solid-water interfaces, Mater. Res. Soc. Bull. 39 (2014) 1056–1061.
- [38] F. Heberling, et al., Reactivity of the calcite-water-interface, from molecular scale processes to geochemical engineering, Appl. Geochem. 45 (2014) 158–190.
- [39] M.P. Andersson, S.L. Stipp, How acidic is water on calcite?, J. Phys. Chem. C 116 (2012) 18779–18787.
- [40] A.G. Evans, Perspective on the development of high-toughness ceramics, J. Am. Ceram. Soc. 73 (1990) 187–206.

- [41] R. Zamora, A. Nair, R. Hennig, D. Warner, Ab initio prediction of environmental embrittlement at a crack tip in aluminum, Phys. Rev. B, Condens. Matter Mater. Phys. 86 (2012).
- [42] R.J. Zamora, K.L. Baker, D.H. Warner, Illuminating the chemo-mechanics of hydrogen enhanced fatigue crack growth in aluminum alloys, Acta Biomater. 100 (2015) 232–239
- [43] P. Andric, W.A. Curtin, New theory for Mode I crack-tip dislocation emission, J. Mech. Phys. Solids 106 (2017) 315–337.

Additional references for supplementary material

- [44] S. Hofmann, K. Voïtchovsky, P. Spijker, M. Schmidt, T. Stumpf, Visualising the molecular alteration of the calcite (104) - water interface by sodium nitrate, Sci. Rep. 6 (2016) 1–11.
- [45] J.H. Rose, J. Ferrante, J.R. Smith, Universal binding energy curves for metals and bimetallic interfaces, Phys. Rev. Lett. 47 (1981) 675–678.
- [46] T. Hong, J.R. Smith, D.J. Srolovitz, J.G. Gay, R. Richter, Determining ab initio interfacial energetics, Phys. Rev. B 45 (1992) 8775–8778.
- [47] G. Henkelman, A. Arnaldsson, H. Jónsson, A fast and robust algorithm for Bader decomposition of charge density, Comput. Mater. Sci. 36 (2006) 354–360.